Available online at www.sciencedirect.com

ScienceDirect

Soils and Foundations 60 (2020) 898–910

www.elsevier.com/locate/sandf

Technical Paper

# Effect of the pore fluid salinities on the behaviour of an electrokinetic treated soft clayey soil

Sara Gargano [a,*], Stefania Lirer [b], Barbara Liguori [c], Alessandro Flora [a]

[a] Department of Civil, Architectural and Environmental Engineering (DICEA), University of Napoli "Federico II", Napoli, Italy
[b] Department of Sustainability Engineering, University "Guglielmo Marconi", Roma, Italy
[c] Department of Chemical, Materials and Industrial Production Engineering (DICMaPI), University of Napoli Federico II, Italy

Received 25 July 2019; received in revised form 26 May 2020; accepted 28 June 2020
Available online 14 August 2020

**Abstract**

Dredging activities of harbours and rivers are becoming very important in many countries all over the world and, as a consequence, the disposal of dredged sediments is a critical concern from an environmental point of view. In order to facilitate the disposal or the reuse of large volume of dredged soils, usually under-consolidated and with a high water content, an electrokinetic treatment can be adopted with the goal to dewater and strengthen the sediments.

This paper presents the results of some electrokinetic tests performed on reconstituted clayey specimens at different pore fluid salinities ($0.2 < s_c < 30$ g/l) treated with electrokinetic (EK) technique. The results indicate that the presence of small quantities of salts in the pore fluid enhances the electro-osmotic consolidation. On the contrary, for high salt concentrations of the pore fluid the electro-osmotic dewatering is significantly reduced. The mechanical behaviour of treated specimens has been investigated at the micro (SEM) and macro scale (triaxial and oedometer tests). The experimental results highlighted the relevant and expected contribution of the pore fluid characteristic on the effectiveness of the treatment as ground improvement technique.


*Keywords:* Electrokinetic treatment; Electro-osmotic consolidation; Oedometer tests; Mechanical behaviour; Clayey soils; Dredged sediments; Microstructure

## 1. Introduction

Dredging of harbours is an activity consisting in the removal of sediments from the seabed to lower it to the depth needed to allow ships docking and operation. This routine activity is becoming increasingly important as larger and larger ships are used. Quite often, a critical issue in the dredging process is the disposal of sediments, because only limited surfaces and volumes are available in most industrialised areas (Van Mieghem et al., 1997). Furthermore, there has been an increasing attention in recent years to the reuse of these sediments to obtain reclaimed land. Whatever the reason why, in most cases it is important to densify the sediments, reducing their volume, eventually improving their mechanical properties.

A persevering management strategy is then necessary in order to reuse dredged sediments (which have the consistency of a slurry) in various soil engineering applications. These sediments need treatments to significantly reduce the high water content, in a cost-efficient way, within a reasonable amount of time.

The three most employed mechanical dewatering techniques (centrifugation, dewatering by belt filter press or filter press) cannot reach a very high dry solid content especially in low permeability fine grained soils, for which it is necessary to find alternative techniques. Among the

Peer review under responsibility of The Japanese Geotechnical Society.
* Corresponding author.
*E-mail address:* sara.gargano@unina.it (S. Gargano).

https://doi.org/10.1016/j.sandf.2020.06.003
0038-0806/

**Nomenclature**

| | | | |
|---|---|---|---|
| $A_c$ | area of the cross section | $s_c$ | salt concentration |
| $c_u$ | undrained cohesion | $t$ | elapsed time |
| $D$ | internal diameter of the device | $v$ | volume of expelled water |
| $e_i$ | initial void ratio | $w_L$ | liquid limit |
| $e$ | current void ratio | $w$ | water content |
| $E$ | energy consumption | $\Delta\Phi$ | electrical potential difference |
| $\bar{E}$ | energy consumption to treat one cubic metre of soil | $\Delta L$ | distance between the electrodes |
| | | $\Delta u$ | pore water pressure increment |
| $E_u$ | undrained Young's modulus | $\varepsilon$ | dielectric constant of the pore fluid |
| $G_s$ | soil specific gravity | $\varepsilon_a$ | axial strain |
| $H$ | height of the device (housing part) | $\rho$ | electrical resistivity |
| $H_s$ | height of the sample | $\sigma'_c$ | effective confining pressure |
| $i$ | current intensity | $\sigma'_e{}^*$ | equivalent vertical stress |
| $i_e$ | electrical potential gradient | $\sigma'_p$ | preconsolidation pressure |
| $k_e$ | coefficient electro-osmotic permeability | $\sigma'_v$ | vertical effective stress |
| $n$ | porosity of the soil | $\sigma'_y$ | yield stress |
| $P$ | power consumption | $\lambda$ | electrical conductivity |
| $q$ | deviatoric stress | $\eta$ | dynamic pore fluid viscosity |
| $q_e$ | flow volume induced by electrical gradient | $\zeta$ | soil zeta potential |
| $R$ | electrical resistance | | |

different options for enhancing sludge dewatering, the application of an electric field has proved to be efficient to remove the water that cannot be removed using mechanical dewatering alone (Gray and Mitchell, 1967; Bjerrum et al., 1967; Fetzer, 1967; Casagrande, 1983; Lockhart, 1983; Chappell and Burton, 1975; Lo et al., 1991; Flora et al., 2016, 2017; Gargano et al., 2019a; Gargano, 2020). Notwithstanding its potential interest for engineering applications, the electrokinetic soil treatment (EK) is still mostly studied at a laboratory scale (Sprute and Kelsh, 1980; Fourie et al., 2007; AbDullah and Al-Abadi, 2010; Mahmoud et al., 2011).

Most of the previous laboratory studies concern the effectiveness of the EK treatment in soil dewatering (Pinzari, 1962; Sprute and Kelsh, 1980; Lockhart, 1983; Tamagnini and Calabresi, 1991; Mohamedelhassan and Shang, 2002; Fourie et al., 2007; Mahmoud et al., 2011; Zhou et al., 2015; Martin et al., 2019). Few studies considered the effectiveness of such technique in the improvement of the soil mechanical properties and the role of some factors affecting the treated soil mechanical behaviour: electrode materials (Xue et al., 2015; Mohamedelhassan and Shang, 2011; Mohamad et al., 2011), current intermittence (Micic et al., 2001), polarity reversal (Melo et al., 2011), preloading (Shang, 1998), drainage direction and room temperature (Tang et al., 2017).

It is well known that a very important parameter that affects the electrokinetic process is the pore fluid salinity (Mohamedelhassan and Shang, 2002). Since sediments can be dredged from different water bodies, the water salinity can change a lot, varying from 0 g/l up to 30 g/l or more. While the role of different salinities of the pore fluid on the dewatering process has been analysed in few studies (Mohamedelhassan and Shang, 2002; Lockhart, 1983), on the contrary its effect on the mechanical behaviour of the treated soil hasn't been studied in literature. For this reason, studies from this perspective could help to understand if the EK treatment can be considered an in-situ ground improvement technique for clayey dredged sediments.

A multidisciplinary research has been developed at the University of Napoli Federico II, in order to analyse the potentiality of the electrokinetic treatment of soils with different pore fluid salinities. The main goal of the paper is to highlight the role of the pore fluid salinities in both the dewatering process and the soil strengthening, being the last aspect not addressed in literature.

The planned experimental activity consists of a series of tests in a special large oedometer apparatus designed at the University of Napoli Federico II (Gargano et al., 2019a; Gargano, 2020) for testing very soft soils under mechanical and electric loading conditions. At the end of all the oedometer tests, some specimens were retrieved from the special apparatus and used for conventional mechanical tests (oedometer and triaxial tests) in order to verify the effectiveness of the EK treatment as ground improvement technique.

## 2. Electrokinetic (EK) treatment

Electrokinetic (EK) mechanisms are activated when the soil is charged with a current (typically a low-voltage direct current). The electrokinetic phenomenon is made up by three different processes, namely electrophoresis, electromigration, and electro-osmosis (Gray and Mitchell, 1967; Casagrande, 1983; Hamed, 1990; Eykholt and Daniel, 1994; Jacobs and Probstein, 1996; Dzenitis, 1996; Abdullah, 2000, 2003). Electrophoresis consists in the migration towards the anode of the negatively charged colloidal particles. Electromigration is the migration of ions (both cations and anions) towards the relative electrode. Finally, electro-osmosis is the water flow that takes place in the diffuse double layer, where there is a high concentration of cations attracted by the negatively charged surface of the clayey particles. When an electrical gradient is applied to the soil, the migration of ions results into a removal of water.

The electromigration of positive ions in the surrounding liquid and in the outer diffused part of the electric double-layer towards the negative electrode (cathode) mechanically draws water, with the result of a movement of liquid in the pores towards the cathode.

The classical equation representing electro-osmotic flow is the one proposed many years ago by Casagrande (1948):

$$q_e = k_e i_e A_c \tag{1}$$

In which $i_e$ is the electrical potential gradient (V/m) that can be expressed as the ratio between the potential difference $\Delta\phi$(V) and the distance between the electrodes $\Delta L$ (m); $k_e$ is the coefficient of electro-osmotic permeability ($m^2/(sV)$) and $A_c$ is the cross section area perpendicular to the water flow ($m^2$).

For the description of the electro-osmotic mechanisms, the Helmholtz-Smoluchowski theory (Gray and Mitchell, 1967, Mitchell, 1993) is often advocated. It is based on the analogy with electrical condensers, assuming that near the surface of soil capillaries wall there are charges of one sign and at a small distance from it there are charges of the other sign, concentrated in a layer.

The water is dragged by the counterions through a mechanism of plug flow. The rate of water flow is controlled by the balance between the electrical force and the friction between the water and the wall. The coefficient of electro-osmotic permeability ($k_e$, eq. (1)) can be then derived (Mitchell, 1993) from such a balance as:

$$k_e = \frac{\zeta \varepsilon \mathrm{n}}{\eta} \tag{2}$$

in which ζ(V) is the soil zeta potential (negative in clayey soils); ε (F/m) is the dielectric constant of the pore fluid; $\eta$(Pa s) the dynamic viscosity of the fluid; $n$ the porosity of the soil.

The coefficient of electro-osmotic permeability $k_e$ is usually considered as a function of only the zeta potential and porosity of the soil, since permittivity and viscosity of the pore water can be considered constant over a wide range of salinity. A large number of researches have been dedicated in the past to the role of water salinity. Some of them indicate that high salinity has an effect to reduce the electro-osmotic flow in the soil (e.g., Casagrande, 1948; Gray and Mitchell, 1967; Mitchell, 1993). Others (Lockhart, 1983; Mohamedelhassan and Shang, 2002) indicate that there is an optimum value of the salt concentration that results into an acceleration of the dewatering rate (0.59 g/l for Lockhart, 1983, and 8 g/l for Mohamedelhassan and Shang, 2002). Several experimental works (Bjerrum et al., 1967; Casagrande, 1949; Lo et al., 1991; Lockhart, 1983; Reddy et al., 2006) have shown that the EK treatment improves the stiffness and strength of soils, also accelerating water expulsion. As obvious, these beneficial effects depend on different factors, like, for instance, soil mineralogy and grading, water characteristics as well as operational conditions (i.e. the applied potential and the type of electrodes).

## 3. Experimental programme

### 3.1. Material properties

The experimental activity has been carried out on a sandy clay with silt (Fig. 1) ($G_s = 2.72$), whose mineralogical composition was evaluated by XRD analysis (Fig. 2) on a powder sample using a PanalyticalX'Pert Pro diffractometer equipped with PixCel 1D detector (operative conditions: CuKα1/Kα2 radiation, 40 kV, 40 mA, 2Θ range from 5 to 80°, step size 0.0131° 2Θ, counting time 40 s per step): the main crystalline phases are quartz (Q), calcite (C), mica (MI) and different clay minerals (CM), such as montmorillonite, chlorite and halloysite.

The soil has high plasticity, it shows a liquid limit ($w_L$) of 0.59 and a plastic limit ($w_P$) of 0.23 when the soil is mixed with distilled water and a liquid limit ($w_L$) of 0.59 and a plastic limit ($w_P$) of 0.22 when the soil is mixed with water with a salinity of 30 g/l.

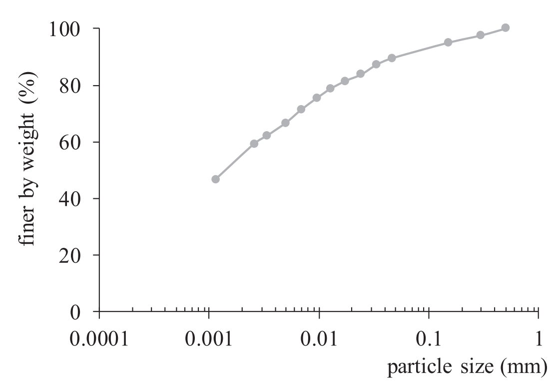


Fig. 1. Grain size distribution of the tested soil.

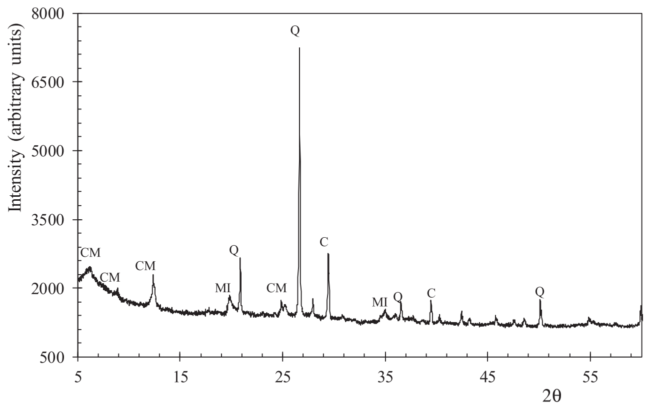


Fig. 2. Mineralogical composition of the soil (CM = clay minerals, MI = mica, Q = quartz, C = calcium carbonate).

### 3.2. Special oedometer

A special floating oedometer (height $H = 25$ cm, internal diameter $D = 6.9$ cm, Fig. 3) has been adopted, to allow large settlements. Different combinations of mechanical (M) and electrical (EK) loads can be applied. The specimen is confined by two graphite porous plates in the device. Graphite has been used, instead of metallic materials, as chemically inert and electrically conducting material to prevent dissolution of the electrode and generation of undesirable corrosion products at the anode in an acidic environment (Alshawabkeh et al., 1999).

The electrical load is applied connecting the plates to a DC power supply, operating under constant voltage ($\Delta\Phi$). During the tests, measurements of settlements (by means of a LVDT), of the weight of water expelled (by means of a scale), and of the intensity of electric current (during the EK tests, by means of a current transducer) were carried out.

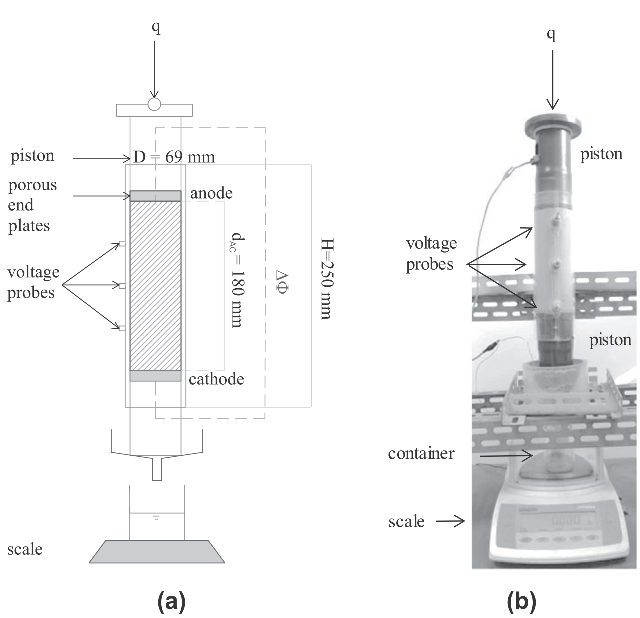


Fig. 3. Experimental device: (a) sketch, (b) picture.

Table 1
Experimental program of the tests carried out in the special oedometer.

| Test | Load (kPa) | $\Delta\phi$ (V) | $s_c$ (g/l) |
|---|---|---|---|
| M1 | 1 | 0 | 0.2 |
| EK1 | 1 | 20 | 0.2 |
| EK2 | 1 | 20 | 8 |
| EK3 | 1 | 20 | 15 |
| EK4 | 1 | 20 | 30 |
| M2 | 30 | 0 | 0.2 |
| EK5 | 30 | 20 | 0.2 |
| EK6 | 30 | 20 | 30 |

### 3.3. Testing programme

All the tests have been carried out on remoulded specimens: the pore fluid (Table 1) was prepared mixing distilled water with different concentrations of sodium chloride (the salt) and then it was mixed with the soil, thus obtaining a sludge with an initial water content equal to 1.4 times the liquid limit $w_L$ (whose value was not affected by water salinity).

The testing programme consists in different kind of tests. At first, special oedometer tests were carried out and then other tests were performed on EK treated specimens with the aim to compare their behaviour with the natural ones (SEM analyses, oedometer and triaxial tests).

Since it hasn't been always possible to retrieve specimens for oedometer and triaxial tests in the same positions within the cylinder (Fig. 3), due to the different conditions of the treated soils, the position of the specimens subjected to the mechanical tests has been reported in the Table 2 together with the initial void ratio ($e_i$). Furthermore, in order to obtain the least disturbed samples, thin-walled stainless steel punches have been used.

Table 2
Experimental program of the mechanical tests carried out at the end of the M and EK tests.

| Test | $\sigma'_c$ (kPa) | $s_c$ (g/l) | $e_i$ | position |
|---|---|---|---|---|
| TX-M1 | 5 | 0.2 | 2.1 | middle-bottom |
| TX-EK1 | 5 | 0.2 | 1.5 | middle-top |
| TX-EK2 | 5 | 8 | 1.8 | middle-top |
| TX-EK3 | 5 | 15 | 2.1 | middle-bottom |
| TX-EK4 | 5 | 30 | 1.4 | middle-top |
| TX-M2 | 30 | 0.2 | 1.5 | middle |
| TX-EK5 | 30 | 0.2 | 1.1 | middle-top |
| TX-EK6 | 30 | 30 | 0.8 | middle-top |
| OED-M1 | – | 0.2 | 1.9 | top |
| OED-EK1 | – | 0.2 | 1.5 | bottom |
| OED-EK2 | – | 8 | 1.7 | bottom |
| OED-EK3 | – | 15 | 1.3 | top |
| OED-EK4 | – | 30 | 2.1 | bottom |
| OED-EK5 | – | 0.2 | 1.6 | bottom |
| OED-EK6 | – | 30 | 1.4 | bottom |

Finally, at the end of the tests some Scanning Electron Microscope analyses have been performed. The specimens were recovered from the middle part in the case of untreated samples and from the anode side in the case of treated samples.

### 3.3.1. Special oedometer apparatus tests

Eight tests have been carried out in the special oedometer (Fig. 3) under a double-way drainage condition (Table 1):

- in two tests (M1 and M2) only a mechanical load (up to $\sigma'_v = 1$ kPa or 30 kPa) has been applied, in particular, to reach 30 kPa subsequent loads were applied until the last step from 15 to 30 kPa;
- in four tests (EK1, EK2, EK3 and EK4) a mechanical load of 1 kPa has been applied together with an electrical field ($\Delta\phi = 20$ V);
- in two tests (EK5 and EK6) subsequent loads were applied until the last step from 15 to 30 kPa where the mechanical load has been applied together with an electrical field ($\Delta\phi = 20$ V).

The electrical field ($\Delta\phi = 20$ V) corresponds to a voltage gradient that goes from 1.1 to 1.4 V/cm, that is perfectly within the range of 0.3 V/cm − 2 V/cm that is commonly used in laboratory tests (Melo et al., 2011, Gargano et al., 2019a, Yang et al., 2019).

The six electrokinetic (EK) tests (Table 1) have been performed with fluid porosity prepared at different salt concentrations ($0.2 < s_c < 30$ g/l, being the boundaries of the range respectively the salt concentration of the tap water and the average salt concentration of the seawater).

During all the tests carried out in the special oedometer many measurements have been collected: volume of expelled water in time, vertical settlements, current intensity and electric potential difference. Furthermore, the coefficient of electro-osmotic permeability, the electrical conductivity and the energy consumption have been calculated.

- Volume of expelled water

In the EK tests, the water flow goes from the top to the bottom of the specimen and is collected at the base by a container placed on a high-resolution scale. The room temperature was controlled and the container on the scale was filled with oil to create a film on the collected water and then covered with a plastic wrap thus preventing the evaporation. Furthermore, since in the mechanical tests (M, with no electric gradient) water is expelled from both the ends of the specimen, this procedure could not be used. However, for saturated specimens the total volume of expelled water can be quantified via the measured settlements, and therefore this more traditional method was used in the M tests.

The expelled volume of water has been chosen, instead of the specimen settlements, because the LVDT data could have been unreliable, because of the unavoidable amount of gas produced by electrolysis during the EK tests (especially at high pore fluid salinities).

The two methods to measure the expelled water (via LVDT and via scale) have been compared during EK tests at low salinities (in which both were adopted), and it was demonstrated that the results are in all similar.

- Coefficient of electro-osmotic permeability

During the EK tests (Table 1) the measurement of expelled water during time allows the calculation of the coefficient of electro-osmotic permeability via eq. (1) ($A_c = 37.4$ cm$^2$, $i_e = 1.1$–$1.4$ V/cm).

- Current intensity and electrical conductivity

The current intensity was measured via amperometer, while the electrical conductivity (that is the reciprocal of electrical resistivity, $\rho$) was evaluated from the current intensity with second Ohm's law, at the beginning of tests and at peak (the maximum).

- Energy consumption

The economic efficiency of the electro-osmotic treatment is evaluated in terms of energy consumption. The power consumption per unit volume of soil ($P$, Watt), is related to the applied electric potential ($\Delta\Phi$, Volts) and to the current intensity ($i$, Ampere):

$$P = \Delta\Phi \cdot i = R \cdot i^2 \tag{3}$$

where $R$ is the electrical resistance (Ohm). The energy consumption, $E$(Wh), is the power consumption (eq. (3)) during the total treatment time ($t$):

$$E = P \cdot t \tag{4}$$

### 3.3.2. SEM analyses

Scanning electron microscopy SEM (SEM, Cambridge S440) analyses have been performed on treated and untreated soils: each dried sample was coated with a thin layer of gold to provide surface conductivity.

To dehydrate the wet soil samples for SEM analysis the freeze-drying technique was performed. One of the most conspicuous problem involving with the assessment of soil fabric is to keep the scanning sample undisturbed. Removing the pore water by traditional methods, such as air or oven drying, can cause a significant shrinkage of the soil with important microstructural changes. The freeze-drying technique allows to minimise soil shrinkage, since a fast freezing of water in the soil pores leads to the formation of non-crystal ice without volume expansion and does not cause deformation to the specimen (Shi et al., 1999). The sample is placed in a freezing unit with a vacuum chamber (Alpha 1–4 LSCplus; −25 °C, 0.1 mbar) and dried by sublimation at a low temperature (−25 °C).

### 3.3.3. Oedometer tests

A conventional oedometer cell with double drainage was used in the OED tests ($H = 20$ mm, $D = 56$ mm). Seven tests (OED-M1, OED-EK1, OED-EK2, OED-EK3, OED-EK4, OED-EK5, OED-EK6, Table 2) have been carried out up to a vertical stress of 5000 kPa with the aim to compare the behaviour of EK treated and untreated specimens (Table 2).

### 3.3.4. Triaxial tests

Some Isotropically Consolidated Undrained Triaxial Tests (CIU tests) have been carried out on specimens retrieved from the special oedometer ($D = 36$ mm, $H = 72$ mm), at the end of mechanical (M) and electrokinetic (EK) tests (Table 2). During the consolidation phase, the effective confining pressure ($\sigma'_c$) has been chosen equal or similar to the maximum vertical stress applied in the special oedometer, to modify only slightly the initial stress state. Then, a deviatoric load has been applied up to specimen's failure in undrained conditions.

Membrane effect has been taken into account (Fukushima and Tatsuoka, 1984), considering the membrane thickness (0.15 mm). This effect is negligible because the maximum increment of confining pressure caused by the membrane confinement is 0.5 kPa.

## 4. Results and discussion

### 4.1. Volume of expelled water

Fig. 4 shows the test results carried out in the special oedometer. It shows that, at the same stress level (from 0 to 1 kPa or from 15 to 30 kPa), the application of an electric field (tests EK1, EK2, EK3, EK4, Fig. 4a and EK5, EK6, Fig. 4b) enhances the consolidation. There is, in fact, a reduction in the time needed to end the consolidation and a higher volume of expelled water respect to the mechanical case alone (M1 and M2 in the Fig. 4a and 4b respectively).

As mentioned before, the application of an electric field accelerates the water expulsion removing water that cannot be removed using mechanical dewatering alone (Gray and Mitchell, 1967; Bjerrum et al., 1967; Fetzer, 1967; Casagrande, 1983; Lockhart, 1983, Chappell and Burton, 1975; Lo et al., 1991, Flora et al., 2016, 2017; Gargano et al., 2019a; Gargano, 2020). As obvious, this beneficial effect depends on different factors, like for instance the pore fluid salinity. In fact, during the application of the electric field, the salinity affects the quantity of water removed, while it seems to be slightly connected to the velocity of consolidation. In particular, for the range of salinity that has been investigated, it can be said that the lower the salt concentration, the higher the quantity of water removed. The total volume of expelled water, as can be seen in Fig. 4a for example, goes from 35 $cm^3$ (for M1) to 88 $cm^3$ (for EK4) until 167 $cm^3$ (for EK1).

Some studies have indicated that high salinity reduces the electro-osmotic flow (Bjerrum et al., 1967; Casagrande, 1948; Gray and Mitchell, 1967; Lo et al., 1991, Mitchell, 1993, Reddy et al., 2006), while others (Lockhart, 1983; Mohamedelhassan and Shang, 2002) have indicated that there is an optimum value of the salt concentration that results into an acceleration of the dewatering rate (0.59 g/l for Lockhart, 1983, and 8 g/l for Mohamedelhassan and Shang, 2002). It should be also noted that, as pore fluid salinity increases, the inhomogeneity of treatment effects increases, with a higher difference of void ratio between the anode and the cathode sides (Table 2). Alshawabkeh et al. (2004) verified that the electric field, along with a flow of water to the cathode, induces a desaturation front in the soil, that is generated in the anodic area and then moves towards the cathodic area. This is responsible for an inhomogeneous degree of saturation along the axis of the specimen (lower saturation towards the anode), which causes a water flow from the cathode to the anode, in the direction to that caused by the electro-osmotic flow. When the two phenomena equilibrate, the electro-osmotic consolidation ends. The desaturation front is also responsible for the reduction in water flow, that derives from a reduction in the permeability of the soil, since the hydraulic continuity of the soil has been compromised.

### 4.2. Electro-osmotic permeability

Fig. 5 shows the average value of the electro-osmotic permeability normalised by the soil porosity ($n$) over the first 500 min of the EK tests plotted against the pore fluid salinity. It can be noted that the experimental results at 1 kPa are in good agreement with the ones of previous researches (Mohamedelhassan and Shang, 2002) that are also reported in Fig. 5. In order to say the same at 30 kPa, other experimental tests are necessary.

As expected, as the pore fluid salinity increases ($s_c \geq 8$ g/l) the ratio $k_e/n$ decreases, because the zeta potential decreases (this is consistent with the Helmholtz-Smoluchowski model, eq. (2)). When the salinity increases, more $Na^+$ ions are present in the pore fluid. The $Na^+$ ions trap water molecules, and therefore there is less water available to be expelled from the soil. On the contrary if the pore fluid salinity goes from 0.2 to 8 g/l the ratio $k_e/n$ increases (Fig. 5). The latter result can not be explained through the Helmholtz-Smoluchowski model and needs further investigations. When the stress level is higher (30 kPa), the value $k_e/n$ becomes independent from the salinity. The permeability is lower and there is a remarkable difference when $s_c$ is 0.2 g/l. This is probably due to the fact that when the consolidation goes ahead, the void ratio decreases and there is less water available for the EK flow. Then, the velocity of the process is lower and thus $k_e/n$ decreases. Therefore, on one hand a soil saturated with

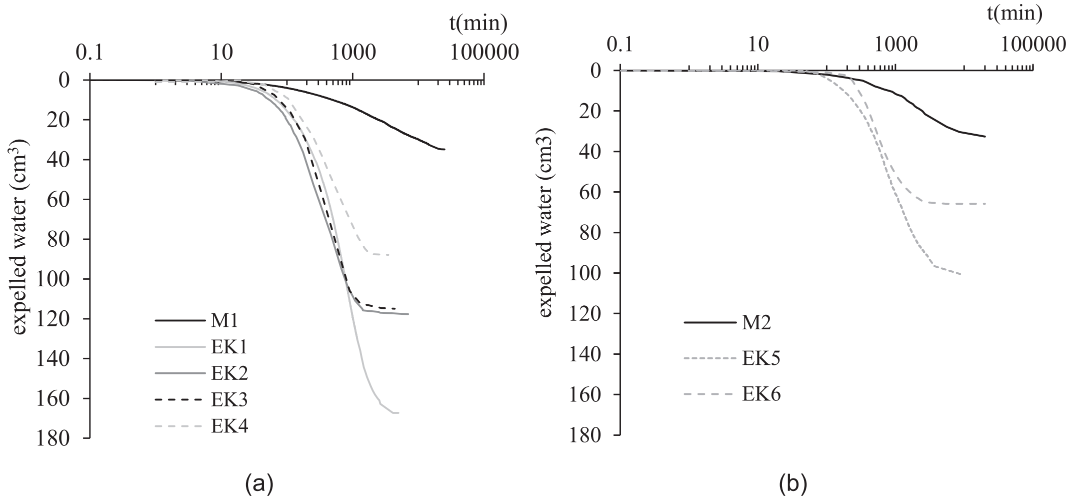


Fig. 4. Volume of water removed during the tests (Tab. 1) versus time at the loading step from 0 to 1 kPa (a) and from 15 to 30 kPa (b).

water with very low salinity (in this case 0.2 g/l) does not necessarily have a high electro-osmotic permeability. On the other, if the pore fluid has a high salinity (in this case 30 g/l), the electro-osmotic permeability is not necessarily very low (Mohamedelhassan and Shang, 2002).

### 4.3. Electrical conductivity

For all the EK tests, the current intensity ($i$) values are higher at the beginning of the tests, and then decrease in time due to the decrease of ionic species in the pore fluid caused by the electro-migration and electro-osmotic flow. In particular, the current intensity reaches its maximum value after 100–200 min. These maximum values are equal to 0.07, 0.19, 0.47 or 0.90 A, while the initial values are equal to 0.066, 0.20, 0.36 or 0.60 A for the salinity of 0.2, 8, 15 or 30 g/l respectively (Table 1).

The conductivity of an electrolyte (the pore fluid) depends on the concentrations of ions: it goes from 0.05 S/m for the tap water to 5 S/m for the seawater, so as

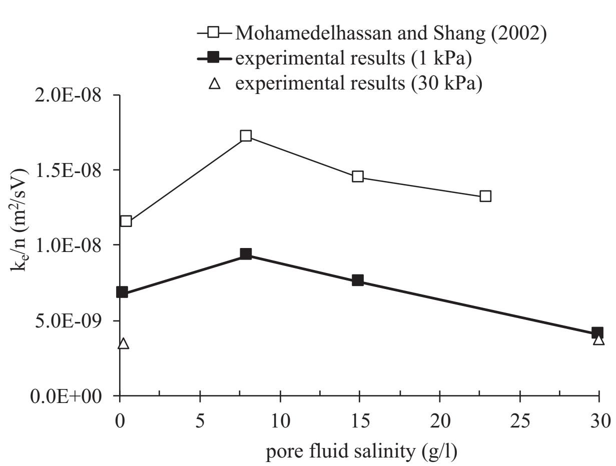


Fig. 5. Coefficient of electro-osmotic permeability normalised by the soil porosity versus the pore fluid salinity.

the salt concentration increases, the current intensity increases too.

The electrical conductivity ($\lambda = i/\Delta\Phi \cdot H_s/A_c$), calculated using the initial and the maximum values of the current intensity and considering the current height of the specimen ($H_s$), have been plotted against the pore fluid salinity in Fig. 6. As expected, it is proportional to the pore fluid salinity and is located between the conductivity of the soil particles, assumed equal to that of a clay with similar geotechnical properties (Mohamedelhassan and Shang, 2002), and the pore fluid conductivity, whose variation with the salinity is known (Keller and Frischknecht, 1966).

### 4.4. Energy consumption

The energy consumption to treat one cubic meter of soil for an hour ($\bar{E}$, Wh/m$^3$) can be used to evaluate quantitatively the feasibility of electro-osmotic treatment in terms of efficiency. It has been calculated via eq. (4), considering the variation of the current intensity with time, and plotted in Fig. 7 against the pore fluid salinity. It is evident that as the higher the pore fluid salinity, the higher the current intensity, the trend is quite the same for the energy consumption.

### 4.5. SEM analyses

Most of soil's properties and characteristics are attributed to its microstructure. Features like pore spaces, clay matrices, and aggregations are demonstrative of soil mechanical properties (such as strength and compressibility). Scanning electron microscopy can be used to recognize microfabric of soils and their microstructures (which constitute macro fabric). Furthermore, all microstructure features like particle arrangements, particle assemblage and pore spaces can be detected (Mirzababaei and Yasrobi, 2007).

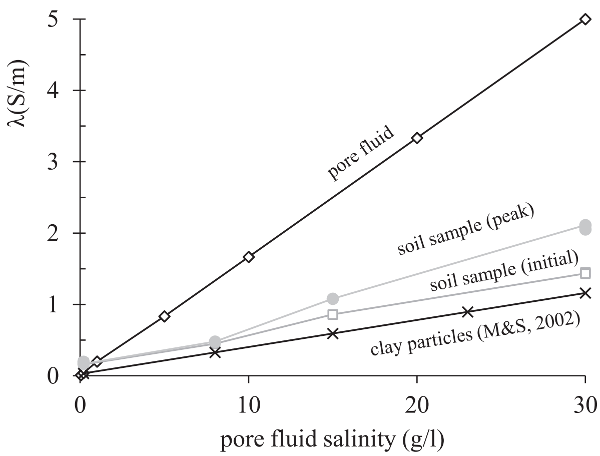


Fig. 6. Electrical conductivity versus pore fluid salinity.

The different behaviour of the specimens in terms of volume change and shear strength seem to be a result of the interaction between salts within the pore fluid and clay particles under the applied electric field. An increase in pore electrolyte concentration can make an edge-face arrangement (typical of a soil formed in a water suspension) transform in a face-face arrangement (typical of a soil in concentrated electrolytes) (van Olphen, 1977; Bennet and Hulbert, 1986; Chen et al., 1990). Furthermore, the thickness of the double layer decreases as salt concentration in the bulk solution increases (Mitchell, 1993; Yong et al., 1992), according to the classical diffuse double layer theory (Gouy, 1910; Chapman, 1913).

Inspecting the SEM images, the untreated soil exhibits an open type microstructure (Fig. 8a), with the platy clay particles assembled in a dispersed arrangement, whereas the EK treated specimen presents some signs of reticulation (Fig. 8b).

As the salt concentration increases (Fig. 9 a-c), the soil particle clusters are interspersed by large openings, thus the flocculated nature of the fabric is more evident

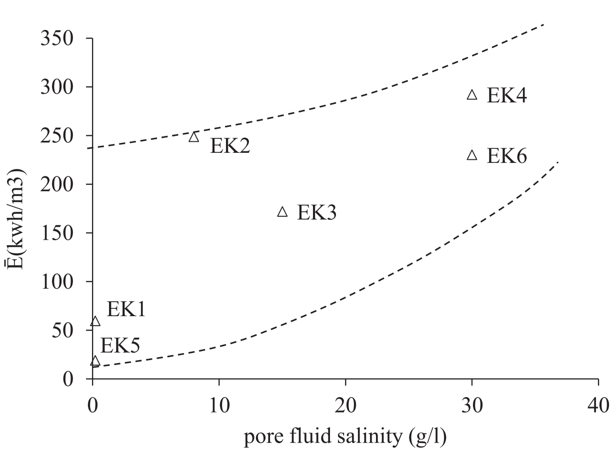


Fig. 7. Energy consumption against pore fluid salinity.

(Gargano, 2020). At the same time, the degree of reticulation seems to increase, and the flatness of the fabric becomes less evident. (Chew et al., 2004). There are highly dense clay matrices and many aggregations. The clay matrices have perturbed parallelism (Mirzababaei and Yasrobi, 2007), the particles appear larger and thicker than those of the untreated soil. Finally, the different applied mechanical vertical stress did not affect the soil fabric (Fig. 10 a and b).

### 4.6. Oedometer tests

Fig. 11 shows the results of the oedometer tests in the semi-logarithmic plane of the void ratio ($e$) versus effective vertical stresses ($\sigma'_v$). For a normally consolidated material, in this plane the normal compression line (NCL) can be identified.

It is known that the electro-osmotic treatment decreases soil water content and increases soil preconsolidation pressure, $\sigma'_p$ (Flora et al., 2017; Gargano, 2020; Rittirong and Shang, 2008). The experimental results indicate that the treated specimens (OED-EK1, OED-EK2, OED-EK3, OED-EK4, OED-EK5, OED-EK6, Fig. 11a and Fig. 11b) have a preconsolidation stress higher (Flora et al., 2017; Gargano, 2020) than that pertaining to the untreated soil (OED-M1). In particular, the soil with electrokinetic treatment is quite stiff at low stress levels, with a compression curve that plots to the right of the one pertaining to the untreated soil, tending to it at high stress levels. This can be clearly seen when the salinity is equal to 30 g/l in the OED-EK4 and OED-EK6 tests (Fig. 11a and Fig. 11b) and 0.2 g/l in the test OED-EK5 (Fig. 11b), while in the other cases there are minor effects on the structure of the treated soils (OED-EK3 has a different behaviour because it was recovered at the anode side, Table 2).

The yield stress ($\sigma'_y$) of the treated clay from the OED tests (Fig. 11b) is about 20 kPa, 90 kPa and 100 kPa for the tests OED-EK4, OED-EK5 and OED-EK6 respectively, much higher than the equivalent vertical stress ($\sigma'_e$*) required to bring the untreated soil (OED-M1) to the same void ratio (1 kPa, 7.5 kPa and 20 kPa, respectively). It is well known that the stress ratio $\sigma'_y$/$\sigma'_e$* is a measure of the effect of structure (Cotecchia and Chandler, 1997), which in this case has been generated by the EK treatment. Since the yield stress of the treated soil exceeds the preconsolidation stress ($\sigma'_p$ was 1 for OED-EK4 and 30 kPa for OED-EK5 and OED-EK6), it lies to the right of the normal consolidation line (NCL). The ratio $\sigma'_y$/$\sigma'_e$* has increased to 20, 12 and 5 for tests OED-EK4, OED-EK5 and OED-EK6, respectively.

During virgin yielding, the structured soils are generally more compressible than the reconstituted ones (Liu and Carter, 1999). As previously mentioned, they tend to the normal compression line of the reconstituted soil at high stresses, because of the progressive destructuration.

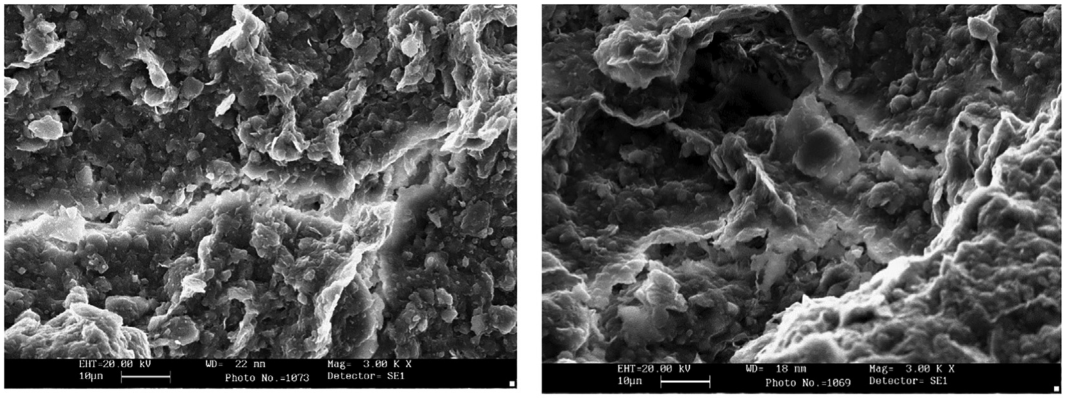

**(a)** **(b)**

Fig. 8. Micrographs of (a) untreated sample M1 and (b) treated sample EK1 at the anode side.

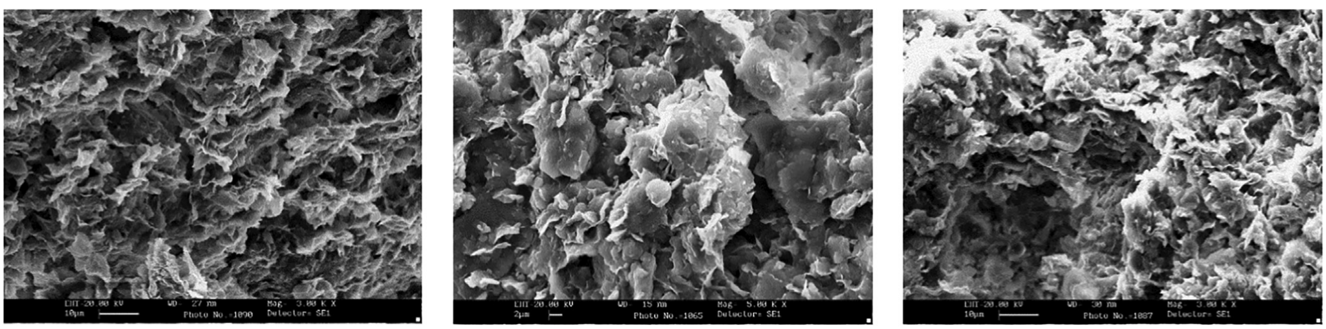

(a) (b) (c)

Fig. 9. Micrographs of treated sample at the anode side: (a) EK2, (b) EK3 and (c) EK4.

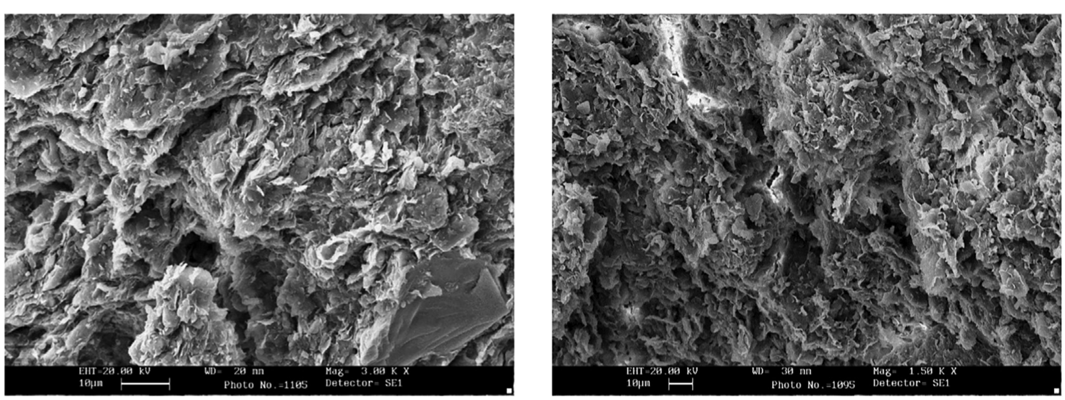

(a) (b)

Fig. 10. Micrographs of treated sample at the anode side: (a) EK5 and (b) EK6.

### 4.7. Triaxial tests

The results of the CIU tests are plotted in Figs. 12 and 13 in terms of deviatoric stress ($q$) versus the axial strain ($\varepsilon_a$) (Fig. 12a and Fig. 13a) and pore water pressure increment ($\Delta u$) versus the axial strain (Fig. 12b and Fig. 13b). The comparisons have been made among results of triaxial tests on specimens at the same effective confining pressure and different pore fluid salinity (Figs. 12 and 13, Table 2). It can be seen that, at the same effective confining stress, the treated specimens always show a higher deviatoric stress (from 2.4 to 8.3 times higher, Fig. 12a or 1.5 times higher, Fig. 13a) than the untreated ones.

At low salt concentrations, positive excess pore pressures develop during the loading phase, consistently with the natural specimen (TX-M1). For highest salt concentration (TX-EK4, with a salinity of 30 g/l), a different behaviour has been observed with the development of

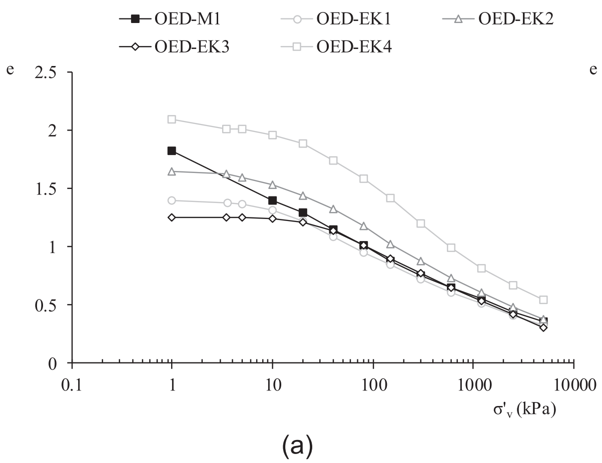


Fig. 11. Results of oedometer test: void ratio – vertical effective stress plane: comparison between tests at different pore fluid salinity (a) and different maximum vertical stress at the same pore fluid salinity (b).

negative excess pore pressures (Fig. 12b). The specimens consolidated at 30 kPa (TX-M2, TX-EK5 and TX-EK6, Fig. 13a and b) show positive pore pressures. Furthermore, TX-EK6 shows a higher deviatoric stress than TX-EK5 (Fig, 12b) but it is quite similar to the one of TX-EK4 test (Fig. 12a), even if the effective confining pressures (Table 2) are different. This means that the specimen TX-EK4 demonstrates higher shear strength without significant decreases in water content (Micic et al., 2001) (TX-EK4 void ratio is 2.1 in opposite to 1.4 for the test TX-EK6, Table 2) and that the EK effect is no longer visible at higher effective confining pressure (30 kPa for the test TX-EK6).

This can also be shown in the plane $c_u$-$w$ (Fig. 14). The fall cone test has been previously used (Gargano et al., 2019b) to estimate the relationship $c_u$-$w$ for the natural soil (continuous black curve), in order to have a quick estimation of the effect of electrokinetic treatment on the mechanical properties of the soil. The tx results have been also shown on the chart. In particular, some relationships can be qualitatively drawn to represent the behaviour of specimens at different positions, pore fluid salinities and stress levels.

It is evident that, some EK treated specimens exhibit higher undrained shear strength after the treatment (dotted lines), with values of $c_u$ above the ones pertaining at the same water content of the untreated specimens (continuous black curve).

The initial value of the secant undrained Young's modulus ($E_u = q/\varepsilon_a$) is plotted against the pore fluid salinity in Fig. 15. As for the coefficient of electro-osmotic permeability ($k_e$), $E_u$ decreases with the salinity when the pore fluid salinity is greater than 8 g NaCl/l while it increases when the pore fluid salinity is between 0.2 and 8 g/l.

## 5. Effectiveness and efficiency

The effectiveness and the efficiency of the EK treatment (Fig. 16) may be evaluated expressing the energy consumption connected to the dewatering rate (represented by the coefficient of the electro-osmotic permeability divided by

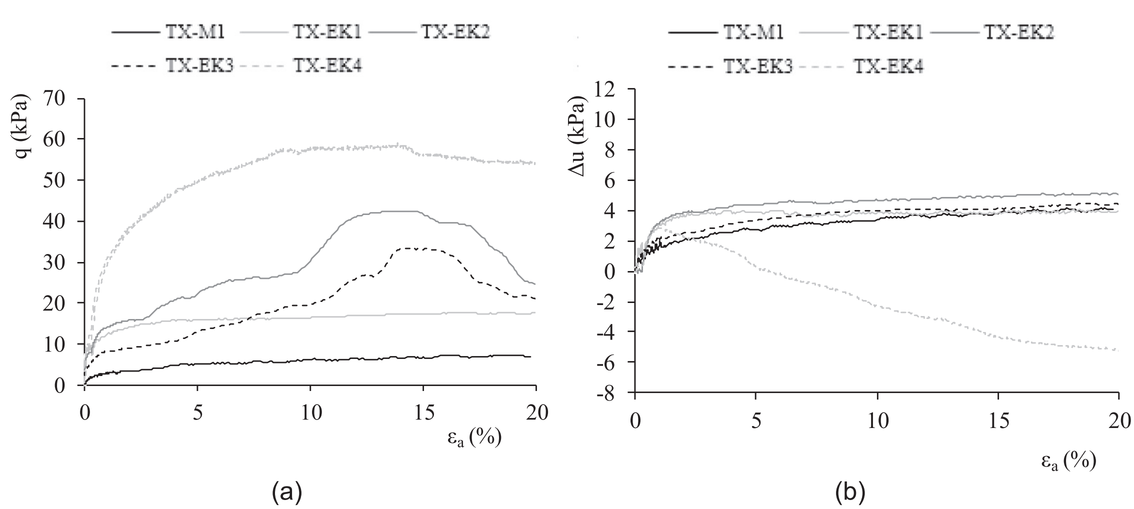


Fig. 12. Results of triaxial tests at $\sigma'_c$ = 5 kPa: deviatoric stress versus axial strain (a) and pore water pressure increment versus axial strain (b).

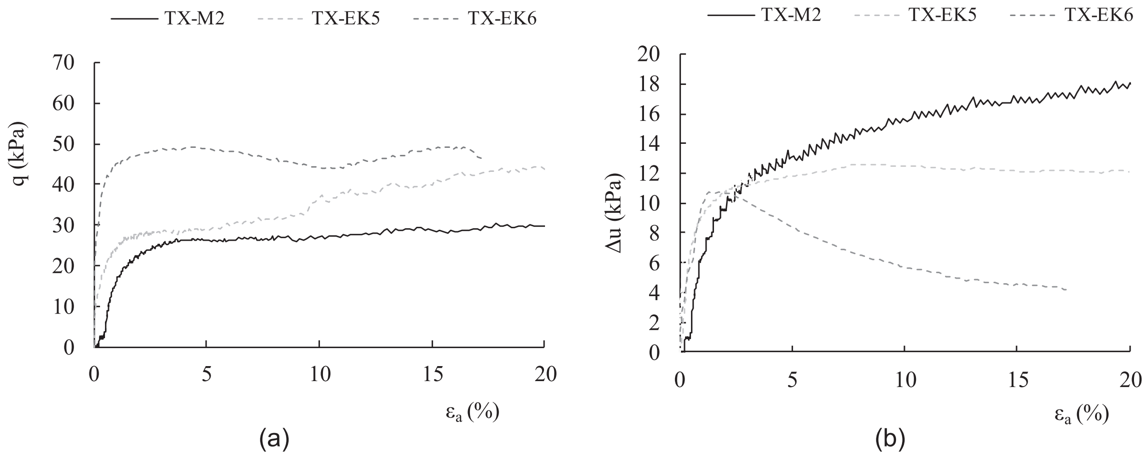


Fig. 13. Results of triaxial tests at $\sigma'_c = 30$ kPa: deviatoric stress versus axial strain (a) and pore water pressure increment versus axial strain (b).

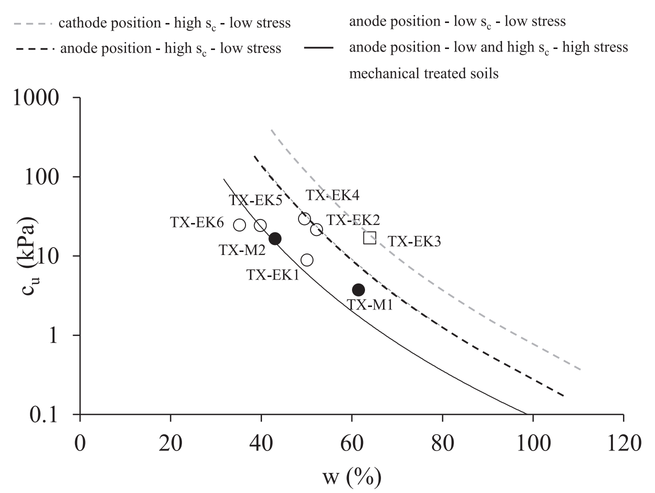


Fig. 14. Relationship between undrained shear strength ($c_u$) and water content ($w$).

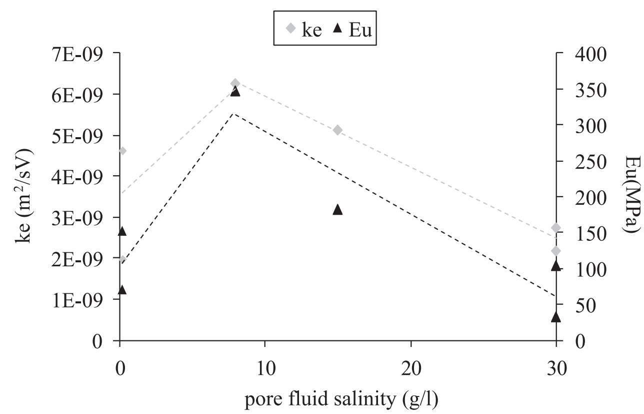


Fig. 15. Coefficient of electro-osmotic permeability and undrained Young's modulus versus the pore fluid salinity.

the porosity) and the mechanical improvement (represented by the undrained cohesion divided by the effective confining pressure).

As at a level stress of 30 kPa the active mechanisms seem to be different and there is a need of more investigations, only the tests at 1 kPa have been considered in the following argument.

As previously discussed, the optimum $k_e/n$ is obtained at the pore fluid salinity of 8 g/l (EK2), while the energy consumption is not the highest. In fact, being strongly connected to the salinity, the energy consumption reaches the maximum at 30 g/l (EK4) where the ratio $c_u/\sigma'_c$ is three times the one of the 0.2 g/l case (EK1).

Furthermore, at 30 g/l (EK4), even if the coefficient of electro-osmotic permeability ($k_e$) is the lowest (so is the dewatering) and the energy consumption is the highest, the treated soil shows a better behaviour in terms of undrained shear strength (the $c_u/\sigma'_c$ values are always higher than the value pertaining to the untreated soil which is 0.7). This is obviously related to the lower value of the void ratio (for EK4 is 1.4, Table 2) induced by electro-osmosis, but the improvement in the mechanical behaviour of soil is not dependent on electro-osmotic consolidation alone. It relies on the chemical and physical reactions that occur during the electro-osmotic process (Estabragh et al., 2014).

Furthermore, the normalised undrained cohesion increases with the salt concentration (since energy consumption in turn increases with the pore fluid salinity, Fig. 7).

## 6. Conclusion

Several laboratory tests were conducted using different pore fluid salinities to provide deep insights into the influence of different pore fluid salinities on the EK treatment, analysing the treated soil at the micro (SEM) and macro scale (mechanical tests).

The electro-osmotic process accelerates the water discharge and increases the volume of expelled water in a way that depends on the pore fluid salinity: it can be said that, for the pore fluid salinities investigated, the lower the salt concentration, the higher the quantity of removed water.

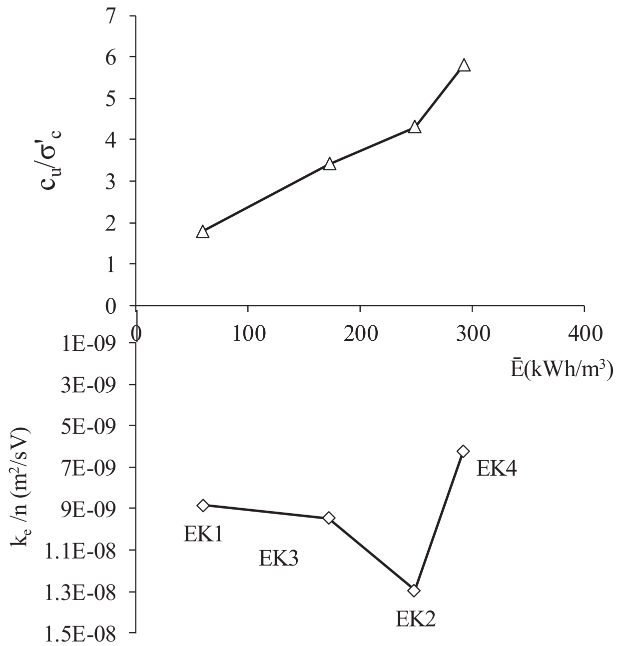


Fig. 16. Coefficient of electro-osmotic permeability normalised by the soil porosity and undrained cohesion normalised by the effective confining pressure against the energy consumption.

The experimental results also show that the EK treatment has a remarkable positive effect on the mechanical behaviour of the treated soil, which exhibits higher shear strength of the untreated soil. This is caused by the structure induced by the treatment, that fades away at high stress levels. Such a structure may be seen as causing a sort of double porosity system, in which the single cluster of clayey particles have a disordered internal microstructure (with a higher void ratio, that collapses when structure is destroyed by high stresses) but the external, macro porosity among the cluster is reduced, with an overall beneficial effect as long as the cluster exist. Regarding the mechanical properties of the treated specimens, the experimental study highlights that such beneficial effect increases as the pore fluid salinity increases.

Further researches are under development to deepen the role of low salt contents that has not been considered in this phase of the research.

## References


Abdullah, W.S., 2000. Electrokinetic Purging of Hexavalent Chromium from Contaminated Soils. Sultan Qaboos University, Muscat, 4–7 March, pp. 444–455.

Abdullah, W.S. (2003). Physico-Chemical Picture and Interpretation of Swell Potential of Expansive Soils and Methods of Stabilization. In Proceedings of the International Conference on Problematic Soils 1. Nottingham Trent University, Nottingham, U.K, 29–30 July, pp. 145–152.

AbDullah, W.S., Al-Abadi, A.M., 2010. Cationic–electrokinetic improvement of an expansive soil. Appl. Clay Sci. 10, 343–350.

Alshawabkeh, A.N., Yeung, A.T. and Bricka, M.R. (1999). Practical Aspects of in Situ Electrokinetic Extraction. Journal of Environmental Engineering: ASCE, 125, 27-35. http://dx.doi.org/10.1061/(ASCE)0733-9372(1999)125:1(27)

Alshawabkeh, A.N., Sheahan, T.C., Wu, X., 2004. Coupling of electrochemical and mechanical processes in soils under DC fields. Mech. Mater. 36 (5–6), 453–465. https://doi.org/10.1016/S0167-6636(03)00071-1.

Bennet, R.H., Hulbert, M.H., 1986. Clay microstructure. Ridel, Dordrecht.

Bjerrum, L., Moum, J., Eide, O., 1967. Application of electro-osmosis to a foundation problem in Norwegian quick clay. Géotechnique 17, 214–235. https://doi.org/10.1680/geot.1967.17.3.214.

Casagrande, L. (1948). Electro-osmosis. In Proceedings, 2nd International Conference on Soil Mechanics and Foundation Engineering, Rotterdam, 1, 218–223.

Casagrande, L., 1949. Electro-osmosis in soils. Géotechnique 1 (3), 159–177. https://doi.org/10.1680/geot.1949.1.3.159.

Casagrande, L., 1983. Stabilization of soils by means of electro-osmosis, state-of-the-art. Geotechnical section of the Boston Society of Civil Engineers- ASCE 69, 255–302.

Chapman, D.L., 1913. A contribution to the theory of electrocapillarity. Phil. Mag. 25 (6), 475±481.

Chappell, B.A., Burton, P.L., 1975. Electro-osmosis applied to unstable embankment. J. Soil Mech. Found. Division ASCE 101 (8), 733–740.

Chen, J.S., Cushman, J.H., Low, P.F., 1990. Rheological behaviour of Na-montmorillonite suspensions at low electrolyte concentration. Clays Clay Miner. 38 (1). https://doi.org/10.1346/CCMN.1990.0380108, 57±62.

Chew, S.H., Kamruzzaman, A.H.M., Lee, F.H., 2004. Physicochemical and engineering behaviour of cement treated clays. J. Geotech. Geoenviron. Eng. 130 (7), 696–706.

Cotecchia, F., Chandler, R.J., 1997. The influence of structure on the pre-failure behaviour of a natural clay. Géotechnique 47 (3), 623–1544. https://doi.org/10.1680/geot.1997.47.3.523.

Dzenitis, J.M., 1996. Soil Chemistry and Flow Prediction in Remediation of Soils by Electric Field Ph.D. Thesis. Massachusetts Institute of Technology MIT.

Estabragh, A.R., Naseha, M., Javadi, A.A., 2014. Improvement of clay soil by electro-osmosis technique. Appl. Clay Sci. 95, 32–36.

Eykholt, G.R., Daniel, D.E., 1994. Impact of system chemistry on electro-osmosis in contaminated soil. J. Geotechnical Engineering, ASCE 120, 797–815.

Fetzer, C.A., 1967. Electro-osmotic stabilization of West Branch Dam Journal of the Soil Mechanics and Foundations Division ASCE 93 (SM4), 85–106.

Flora, A., Gargano, S., Lirer, S., Mele, L., 2016. Effect of Electrokinetic consolidation on fine grained dredged sediments. VI national conference of researchers in geotechnical engineering (CNRIG), Italy. Procedia Eng. 158 (2016), 3–8. https://doi.org/10.1016/j.proeng.2016.08.396.

Flora, A., Gargano, S., Lirer, S., Mele, L., 2017. Experimental evidences of the strengthening of dredged sediments by electro-osmotic consolidation. Geotech. Geol. Eng. 35 (6), 2879–2890. https://doi.org/10.1007/s10706-017-0286-9.

Fourie, A.B., Johns, D.G., Jones, C.J.F.P., 2007. Dewatering of mine tailings using electrokinetic geosynthetics. Canadian Geotech. J. 44, 160–172. https://doi.org/10.1139/T06-112.

Fukushima, S., Tatsuoka, F., 1984. Strength and deformation characteristics of saturated sand at extremely low pressures. Soils Found. 24 (4), 30–48.

Gargano, S., Lirer, S. and Flora, A. (2019a). Analysis of the coupled electro-osmotic and mechanical consolidation in clayey soils. Proceedings of the Institution of Civil Engineers - Ground Improvement172 (3): 146-157. https://doi.org/10.1680/jgrim.18.00010.

Gargano S, Lirer S, Liguori B, and Flora A (2019b). Experimental analysis of the effects of electrokinetic treatment of soils. E3S Web of Conferences 92, 11020 (2019). 7th International Symposium on Deformation Characteristics of Geomaterials, Glasgow 2019.

Gargano, S, 2020. Experimental and numerical study of the behaviour of unconsolidated soils and of the effectiveness of electrokinetic treatment. PhD Thesis. University of Naples, Italy.

Gouy, G., 1910. Charge électrique la surface d'un electrolyte. J. Phys. (Paris) IV No. 9, 457±468.

Gray, D.H., Mitchell, J.K., 1967. Fundamental aspects of electro-osmosis in soils. J. Soil Mechanics and Foundations Division ASCE 93 (6), 209–236.

Hamed, J. (1990). Decontamination of Soil using Electro-osmosis. Louisiana State University in Partial Fulfilment of the Degree of Doctor of Philosophy, Dissertation.

Jacobs, R.A., Probstein, R.F., 1996. Two-dimensional modelling of electroremediation. AIChE J. 42, 1685–1696.

Keller, G.V., Frischknecht, F.C., 1966. Electrical methods in geophysical prospecting. Pergamon Press, Oxford, 517 ss.

Liu, M.D., Carter, J.P., 1999. Virgin compression of structured soils. Géotechnique 49 (1), 43–57. https://doi.org/10.1680/geot.1999.49.1.43.

Lo, K.Y., Ho, K.S., Inculet, I.I., 1991. Electro-osmotic strengthening of soft sensitive clays. Can. Geotech. J. 28, 62–73. https://doi.org/10.1139/t91-007.

Lockhart, N.C., 1983. Electro-osmotic dewatering of clays, II. Influence of salt, acid and flocculants. Colloids Surf. 6, 253–269.

Mahmoud, A., Olivier, J., Vaxelaire, J., Hoadley, A.F.A., 2011. Electro-dewatering of wastewater sludge: influence of the operating conditions and their interactions effects. Water Res. 45, 2795–2810. https://doi.org/10.1016/j.watres.2011.02.029.

Martin, L., Alizadeh, V., Meegoda, J., 2019. Electro-osmosis treatment techniques and their effect on dewatering of soils, sediments, and sludge: A review. Soils Found. 59 (2), 407–418. https://doi.org/10.1016/j.sandf.2018.12.015.

Melo C.M.A.R., Tibana S., Saboya F., Reis R.M., Del Aguila V.M., and da Silva E. Z. (2011). Physical models consolidation by electro-osmosis. In: 14° Panamerican Conference on Soil Mechanics and Geotechnical Engineering, Toronto. Pan-Am CGS Geotechnical Conference.

Micic, S., Shang, J.Q., Lo, K.Y., Lee, Y.N., Lee, S.W., 2001. Electrokinetic strengthening of a marine sediment using intermittent current. Can. Geotech. J. 38 (2), 287–302. https://doi.org/10.1139/t00-098.

Mirzababaei, M. and Yasrobi, S. (2007). Assessment of clay soil fabric using scanning electron microscope (SEM). In First Sri Lankan Geotechnical Society (SLGS) International Conference on soil and Rock Engineering, Colombo, Sri Lanka.

Mitchell, J.K., 1993. Fundamentals of Soil Behaviour, 2nd ed. Wiley, New York.

Mohamedelhassan, E., Shang, J.Q., 2002. Feasibility assessment of electro-osmotic consolidation on marine sediment. Ground Improvement 6 (4), 145–152. https://doi.org/10.1680/grim.2002.6.4.145.

Mohamedelhassan, E., Shang, J.Q., 2011. Effects of electrode materials and current intermittence in electro-osmosis. Ground Improvement 5 (1), 3–11.

Mohamad, E.T., Othman, M.Z., Adnan, S.S., 2011. The effectiveness of electrodes types on electro-osmosis of malaysian soil. Electronic J. Geotechnical Engineering 16, 887–898.

Pinzari, U., 1962. Indagine sul trattamento elettrosmotico di un materiale argilloso. Rivista Italiana di Geotecnica (RIG) 9 (3), 101–114.

Reddy, K.R., Urbanek, A., Khodadoust, A.P., 2006. Electro-osmotic dewatering of dredged sediments: Bench-scale investigation. J. Environ. Manage. 78, 200–208. https://doi.org/10.1016/j.jenvman.2005.04.018.

Rittirong, A., Shang, J.Q., 2008. Numerical analysis for electro-osmotic consolidation in two-dimensional electric field. Proceedings of the Eighteenth (2008) International Offshore and Polar Engineering Conference.

Shang, J.Q., 1998. Electro-osmosis-enhanced preloading consolidation via vertical drains. Can. Geotech. J. 35, 491–499. https://doi.org/10.1139/t98-018.

Shi, B., Wu, Z., Inyang, H., Chen, J., Wang, B., 1999. Preparation of soil specimens for SEM analysis using freeze-cut-drying. Bull. Eng. Geol. Environ. 58 (1), 1–7. https://doi.org/10.1007/s100640050064.

Sprute, R. H. and Kelsh, D.J. (1980). Dewatering fine-particle suspensions with direct current. In Proceedings of the international symposium of fine particle processing, Las Vegas, Nev., vol 2, 1828–1844

Tamagnini, C., Calabresi, G., 1991. Esperienze sul consolidamento elettrosmotico di terreni argillosi teneri. Rivista Italiana di Geotecnica (RIG) 25 (2), 115–136.

Tang, X., Xue, Z., Yang, Q., Li, T., Van Severen, M., 2017. Water content and shear strength evaluation of marine soil after electro-osmosis experiments. Drying Technol. 35 (14), 1696–1710. https://doi.org/10.1080/07373937.2016.1270299.

Xue, Z., Tang, X., Yang, Q., Wan, Y., Yang, G., 2015. Comparison of electro-osmosis experiments on marine sludge with different electrode materials. Drying Technol. 33 (8), 986–995.

Van Mieghem, J., Smits, J., Sas, M., 1997. Large-scale Dewatering of Fine-grained Dredged Material. Terra et Aqua, 21–28.

Van Olphen, H., 1977. An introduction to clay colloid chemistry, 2nd edn. Wiley Interscience, New York.

Yang, S., Jianting, F., Wen, S., Chenchen, Q., 2019. Effects of voltage gradients on electro-osmotic characteristics of taizhou soft clay. Int. J. Electrochem. Sci. 14, 2136–2159 https://doi.org/10.20964/2019.03.06.

Yong, R.N., Mohamed, A.M.O., Warkentin, B.P., 1992. Principles of contaminant transport in soils. Elsevier, Amsterdam.

Zhou, J., Li, T.Y., Xu, C., Nan, G.X., Chuan, H.P., 2015. Electro-osmotic strengthening of silts based on selected electrode materials. Soils Found. 55 (5), 1171–1180. https://doi.org/10.1016/j.sandf.2015.09.017.